Fragility of Charge Order Near an Antiferromagnetic Quantum Critical Point

Xiaoyu Wang, Yuxuan Wang, Yoni Schattner, Erez Berg, and Rafael M. Fernandes

Phys. Rev. Lett. **120**, 247002 — Published 15 June 2018

DOI: 10.1103/PhysRevLett.120.247002

Is charge order induced near an antiferromagnetic quantum critical point?

Xiaoyu Wang,[1,2] Yuxuan Wang,[3] Yoni Schattner,[4,5,6] Erez Berg,[2] and Rafael M. Fernandes[1]

[1] *School of Physics and Astronomy, University of Minnesota, Minneapolis, MN 55455*
[2] *Department of Physics, University of Chicago, Chicago, IL 60637*
[3] *Institute for Condensed Matter Theory and Department of Physics, University of Illinois, Urbana-Champaign, IL 61801*
[4] *Weizmann Institute of Science, Rehovot 761000, Israel*
[5] *Department of Physics, Stanford University, Stanford, California 94305, USA*
[6] *Stanford Institute for Materials and Energy Sciences, SLAC National Accelerator Laboratory and Stanford University, Menlo Park, CA 94025, USA*

We investigate the interplay between charge order and superconductivity near an antiferromagnetic quantum critical point using sign-problem-free Quantum Monte Carlo simulations. We establish that, when the electronic dispersion is particle-hole symmetric, the system has an emergent SU(2) symmetry that implies a degeneracy between d-wave superconductivity and charge order with d-wave form factor. Deviations from particle-hole symmetry, however, rapidly lift this degeneracy, despite the fact that the SU(2) symmetry is preserved at low energies. As a result, we find a strong suppression of charge order caused by the competing, leading superconducting instability. Across the antiferromagnetic phase transition, we also observe a shift in the charge order wave-vector from diagonal to axial. We discuss the implications of our results to the universal phase diagram of antiferromagnetic quantum-critical metals and to the elucidation of the charge order experimentally observed in the cuprates.

The phase diagrams of a number of strongly correlated materials display putative quatum critical points (QCP), in which the transition temperature of an electronically ordered state is suppressed to zero. In systems displaying antiferromagnetic (AFM) order, such as heavy fermions, cuprates, and iron pnictides, unconventional superconductivity (SC) is found to emerge near the QCP [1]. Although it is well established that the interactions mediated by fluctuations near an AFM-QCP favor a sign-changing SC gap, the extent to which this physics describes the actual materials remains widely debated. In this context, analytical investigations of metallic AFM-QCP in two dimensions revealed a surprising result: the same electronic interaction that promotes sign-changing SC also promotes an unusual sign-changing bond charge order (CO) [2–6]. This magnetic mechanism for CO is sharply distinct from the usual mechanisms involving phonons and Fermi surface nesting. Taken at face value, this result would suggest that CO should emerge generically in the phase diagrams of AFM systems.

These theoretical results were brought to the spotlight by the experimental observation of sign-changing bond CO in cuprate high-T_c superconductors [7–19], spurring many ideas on the interplay between AFM-QCP, SC, and CO [5, 6, 20–26]. It has been proposed, for instance, that the pseudogap physics is a manifestation of a more fundamental symmetry between SC and CO near an AFM-QCP [4]. However, most of these theoretical works have relied on certain uncontrolled approximations, which are required for an analytical treatment of an AFM-QCP in a metal. The fundamental question about the universality of CO near an AFM-QCP, and the more specific question about the relevance of this result to explain charge order in cuprates, beg for unbiased methods to probe this phenomenon.

In this paper, we employ the determinantal Quantum Monte Carlo (QMC) method to address these questions. We consider the two-band version of the spin-fermion model, for which the QMC does not suffer from the fermionic sign-problem [27]. The model consists of free electrons coupled to an AFM order parameter tuned to its QCP [28]. Analytical and sign-problem-free QMC calculations have established the existence of a SC dome surrounding the QCP [28, 29]. As for CO, an emergent SU(2) symmetry between CO and SC was found analytically within an approximation that considers only the vicinity of the AFM hot spots – the points on the Fermi surface separated by the AFM wave-vector $\mathbf{Q}_{\rm AFM} = (\pi, \pi)$ [3, 4]. The resulting CO wave-vector lies along the diagonal of the Brillouin zone, $\mathbf{Q}_{\rm CO} = (Q_0, Q_0)$, with $\sqrt{2}Q_0$ being the distance between hot spots. CO with axial wave-vectors $(Q_0, 0)$ and/or $(0, Q_0)$, which are those experimentally observed in cuprates, has also been proposed within the spin-fermion model [5, 30, 31]. Although QMC investigations have not yet found CO, they have focused on very narrow parameter regimes [29], or were performed in the superconducting phase [32].

Here, we report QMC results showing the existence of an SU(2) symmetry between CO and SC near the AFM-QCP when the non-interacting band structure has particle-hole symmetry. This SU(2) symmetry implies a degeneracy between SC and CO, manifested by a sharp enhancement of both susceptibilities as the QCP is approached. This result demonstrates the non-trivial mechanism of magnetically-mediated CO, and establishes that the same interaction that promotes SC in the spin-fermion model is also capable of promoting CO.

As the particle-hole symmetry is broken, however, we

find that while the enhancement of the SC susceptibility is preserved, the CO susceptibility shows a very weak enhancement near the QCP. Furthermore, near the onset of SC, the CO susceptibility is even suppressed with respect to its non-interacting value, signaling a strong competition between these two states already in the fluctuating regime. This happens even though the SU(2) symmetry is preserved locally at the hot spots. The fragility of the CO-SC degeneracy implies that CO near an AFM-QCP is not a universal phenomenon, but instead requires a fine-tuned band structure that goes beyond just hot-spot properties. We also investigate the wave-vector for which the CO susceptibility is maximal. When CO and SC are degenerate, the wave-vector is diagonal, in agreement with the analytical approximations. However, once CO and SC are no longer degenerate, the wave-vector tends to change from diagonal to axial as the AFM phase is approached. This is consistent with theoretical proposals that axial CO is favored over the diagonal one if the anti-nodal region of the Brillouin zone is gapped [33, 34]. Finally, we discuss the implications of our results to materials that display putative AFM-QCPs and their relevance to understand CO in cuprates.

The spin-fermion model is a low-energy model describing electrons interacting via the exchange of AFM fluctuations. In its two-band version (whose physics has been argued to be similar to the one-band version [35]), the model is described by the following action, $S = S_\psi + S_\phi + S_\lambda$, defined on a two-dimensional square lattice:

$$
\begin{aligned}
S_\psi &= \int_{\tau,\mathbf{r}\mathbf{r}'} \sum_{i=c,d} \left[\left(\partial_\tau - \mu\right) \delta_{\mathbf{r}\mathbf{r}'} - t_{i,\mathbf{r}\mathbf{r}'} \right] \psi^\dagger_{i,\mathbf{r}\alpha} \psi_{i,\mathbf{r}'\alpha} \\
S_\phi &= \frac{1}{2} \int_{\tau,\mathbf{r}} \left[\frac{1}{v_s^2} \left(\partial_\tau \boldsymbol{\phi}\right)^2 + \left(\nabla \boldsymbol{\phi}\right)^2 + r_0 \boldsymbol{\phi}^2 + \frac{u}{2} \left(\boldsymbol{\phi}^2\right)^2 \right] \\
S_\lambda &= \lambda \int_{\tau,\mathbf{r}} e^{i\mathbf{Q}_{\mathrm{AFM}}\cdot\mathbf{r}} \boldsymbol{\phi} \cdot \left(\psi^\dagger_{c,\mathbf{r}\alpha} \boldsymbol{\sigma}_{\alpha\beta} \psi_{d,\mathbf{r}\beta} + h.c. \right) \qquad (1)
\end{aligned}
$$

Here, $\int_{\tau,\mathbf{r}}$ is shorthand for $\int d\tau \sum_{\mathbf{r}}$, $\tau \in [0, \beta)$ is the imaginary time, and $\beta = 1/T$ is the inverse temperature. The action S_ψ describes the fermionic degrees of freedom, with the operator $\psi_{i,\mathbf{r}\alpha}$ annihilating an electron of spin α at site $\mathbf{r}$ and band i. Summation over α, β is implied. The two electron bands are labeled c and d. The band dispersion is parametrized by the chemical potential μ and the hopping amplitudes $t_{i,\mathbf{r}\mathbf{r}'}$. Here, we consider only nearest-neighbor hopping and set $t_{c,x} = t_{d,y} \equiv t_x$ and $t_{c,y} = t_{d,x} \equiv t_y$ to enforce the system to remain invariant under a 90° rotation followed by a $c \leftrightarrow d$ exchange. The action S_ϕ describes the spin degrees of freedom, with the bosonic field $\boldsymbol{\phi}$ denoting the AFM order parameter with ordering wave-vector $\mathbf{Q}_{\mathrm{AFM}} = (\pi, \pi)$, and $\boldsymbol{\sigma}$ denoting Pauli matrices. The lattice derivative $(\nabla\boldsymbol{\phi})^2$ is short for $\sum_{\boldsymbol{\delta}=\hat{x},\hat{y}} (\boldsymbol{\phi}_{\mathbf{r}} - \boldsymbol{\phi}_{\mathbf{r}+\boldsymbol{\delta}})^2$. The parameter r_0 tunes the AFM transition, whereas v_s and u describe the stiffness of temporal and amplitude fluctuations respectively. To save computational time, we follow previous works and consider easy-plane antiferromagnetism, i.e $\boldsymbol{\phi} = (\phi_x, \phi_y)$ [29, 35, 36]. The action S_λ couples spins and fermions via the parameter λ. The two-band structure of the model ensures the absence of the sign problem in our simulations [27].

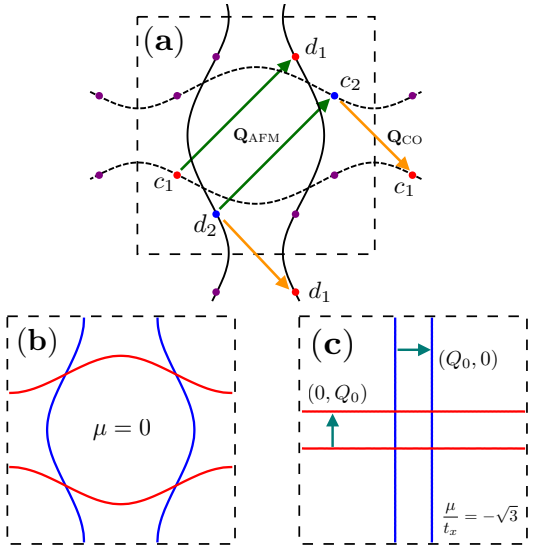

Figure 1. (a) Schematic Fermi surface of the spin-fermion model with two bands (c, dashed line, and d, solid line). Hot spots are marked by solid symbols. Two pairs of hot spots (c_1, d_1) and (c_2, d_2) are highlighted to illustrate the relationship between the AFM wave-vector $\mathbf{Q}_{\mathrm{AFM}}$ and the CO wave-vector $\mathbf{Q}_{\mathrm{CO}}$. The band dispersions used in our QMC calculations are shown in (b) (particle-hole symmetric dispersion, $\mu = 0$, with $t_y = t_x/2$) and (c) (particle-hole asymmetric dispersion, $\mu/t_x = -\sqrt{3}$, with $t_y = 0$). Changing μ tunes the CO wave-vector $\mathbf{Q}_{\mathrm{CO}} = (Q_0, Q_0)$ since $Q_0 = 2 \arccos \frac{-\mu}{2t_x}$.

The fermionic, magnetic, and superconducting properties of this model have been thoroughly studied recently, revealing a SC dome surrounding the QCP [29, 36]. In particular, the SC order parameter Δ was found to have a "d-wave" symmetry, i.e. to change its sign between the two bands: $\Delta = \int_{\tau,\mathbf{r}} i\sigma^y_{\alpha\beta} \left(\psi_{c,\mathbf{r}\alpha} \psi_{c,\mathbf{r}\beta} - \psi_{d,\mathbf{r}\alpha} \psi_{d,\mathbf{r}\beta} \right)$. The CO order parameter ρ investigated here also has opposite signs in the two-bands (and is thus analogous to the d-wave bond CO in the one-band version of the model): $\rho = \int_{\tau,\mathbf{r}} e^{i\mathbf{Q}_{\mathrm{CO}}\cdot\mathbf{r}} \sigma^0_{\alpha\beta} \left(\psi^\dagger_{c,\mathbf{r}\alpha} \psi_{c,\mathbf{r}\alpha} - \psi^\dagger_{d,\mathbf{r}\alpha} \psi_{d,\mathbf{r}\beta} \right)$, where $\mathbf{Q}_{\mathrm{CO}}$ is the CO wave-vector.

Analytical studies found a symmetry relating the SC and CO order parameters under an approximation that focuses on the vicinity of the hot spots [3–5, 37]. In the two-band version of the model, each hot spot of a given pair (c_i, d_i) is located on a different band, as shown in Fig. 1(a). The hot-spots model with linearized dispersions has an emergent SU(2) symmetry that rotates the SC order parameter, $\Delta_{\mathrm{h.s.}} = i\sigma^y_{\alpha\beta} \left(\psi_{c_1,\alpha} \psi_{c_2,\beta} - \psi_{d_1,\alpha} \psi_{d_2,\beta} \right)$, onto the CO order pa-

rameter, $\rho_{\text{h.s.}} = \sigma^0_{\alpha\beta}\left(\psi^\dagger_{c_1,\alpha}\psi_{c_2,\beta} - \psi^\dagger_{d_1,\alpha}\psi_{d_2,\beta}\right)$. This CO has a diagonal wave-vector $\mathbf{Q}_{\text{CO}} \equiv (Q_0, Q_0)$ which separates two hot spots belonging to different pairs but to the same band (see Fig. 1(a)). Our goal here is to investigate: (i) to what extent does this symmetry play a role in the vicinity of an AFM-QCP, and (ii) more broadly, is CO a generic feature near such a QCP. To this end, we perform a systematic investigation of the SC and CO susceptibilities in the two-band spin-fermion model.

We choose as our starting point the parameters for which the approximate SU(2) symmetry is promoted to an exact lattice symmetry. This corresponds to the case where the c and d bands are particle-hole symmetric, i.e. $\mu = 0$. This allows us to systematically study the effect of breaking the particle-hole symmetry at the lattice level. For $\mu = 0$, the electronic action for a given AFM field configuration – corresponding to the S_ψ and S_λ terms of the action in Eq. (1) – is invariant under a rotation in particle-hole space, $\psi_{i\mathbf{r}\alpha} \rightarrow e^{i\mathbf{Q}_{\text{AFM}}\cdot\mathbf{r}}\left(i\sigma^y_{\alpha\beta}\right)\psi^\dagger_{i,\mathbf{r}\beta}$. This invariance can be seen by constructing a four-dimensional spinor that combines rotated and non-rotated operators at each band, $\Psi_{i,\mathbf{r}} \equiv \left(\psi_{i,\mathbf{r}\uparrow},\ \psi_{i,\mathbf{r}\downarrow},\ e^{i\mathbf{Q}_{\text{AFM}}\cdot\mathbf{r}}\psi^\dagger_{i,\mathbf{r}\downarrow},\ -e^{i\mathbf{Q}_{\text{AFM}}\cdot\mathbf{r}}\psi^\dagger_{i,\mathbf{r}\uparrow}\right)^T$. In this representation, when $\mu = 0$, the Hamiltonian commutes with all all SU(2) generators $\boldsymbol{\tau}$ in particle-hole space. Importantly, the SC and CO order parameters form a three-component vector $\boldsymbol{\Phi} \equiv (\mathfrak{Re}\Delta, \mathfrak{Im}\Delta, \rho)$, and couples to the electrons as $\sum_{\mathbf{r}} e^{i\mathbf{Q}_{\text{AFM}}\cdot\mathbf{r}}\boldsymbol{\Phi}\cdot(\sigma_0\otimes\boldsymbol{\tau})\left(\Psi^\dagger_{c,\mathbf{r}}\Psi_{c,\mathbf{r}} - \Psi^\dagger_{d,\mathbf{r}}\Psi_{d,\mathbf{r}}\right)$. Note that $\mathbf{Q}_{\text{CO}} = \mathbf{Q}_{\text{AFM}}$, enforcing ρ to be real. As a result, an enhancement of the SC susceptibility implies an equally strong enhancement in the CO channel. This symmetry is analogous to the that observed in the half-filled negative-U Hubbard model [38]. Here, however, both the SC and CO have a d-wave symmetry.

To demonstrate the existence of this SU(2) symmetry for $\mu = 0$, we perform QMC simulations on a square lattice of size $L = 12$. All energies are expressed in terms of the hopping $t_x \equiv t$ and the parameters are set to $v_s = 2t$, $u = t^{-1}$, $\lambda^2 = 4t$, and $t_y = t/2$, resulting in the Fermi surface shown in Fig. 1(b) (Other particle-hole symmetric dispersions are presented in the Supplementary Material). Fig. 2(a) shows the SC susceptibility χ_{SC}, the CO susceptibility $\chi^{\text{diag}}_{\text{CO}}$ with diagonal wave-vector $\mathbf{Q}_{\text{CO}} = (Q_0, Q_0)$, where $Q_0 = \pi$, and the CO susceptibility $\chi^{\text{axial}}_{\text{CO}}$ with axial wave-vector $\mathbf{Q}_{\text{CO}} = (Q_0, 0)\,/\,(0, Q_0)$ as a function of the distance to the AFM-QCP for $\beta t = 12$. The position r_c of the AFM-QCP is determined via the AFM susceptibility [35]. The degeneracy between diagonal CO and SC is evident, as well as the enhancement of both susceptibilities at the AFM-QCP. The fact that $\chi_{\text{SC}} = 2\chi^{\text{diag}}_{\text{CO}}$ is because the complex SC order parameter has two components whereas the real CO order parameter has one. In contrast, the axial CO susceptibility remains small and nearly unaffected by the proximity to the QCP. Fig. 2(b), which shows the behavior at the QCP, confirms that the degeneracy is present at all temperatures.

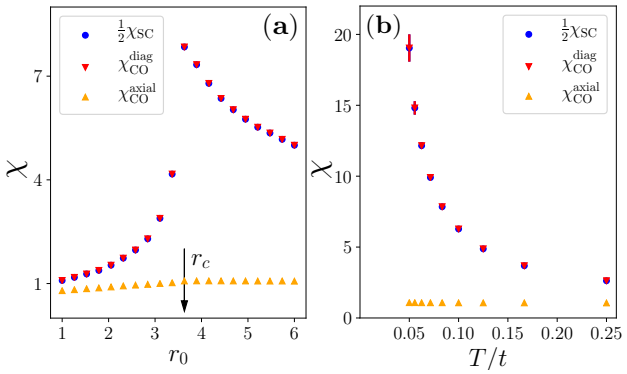

Figure 2. SC susceptibility χ_{SC} (circles) and CO susceptibilities for diagonal wave-vector $\mathbf{Q}_{\text{CO}} = (Q_0, Q_0)$, $\chi^{\text{diag}}_{\text{CO}}$ (triangles), and axial wave-vector $\mathbf{Q}_{\text{CO}} = (Q_0, 0)\,/\,(0, Q_0)$, $\chi^{\text{axial}}_{\text{CO}}$ (inverted triangles), as function of: (a) the distance $r_0 - r_c$ to the AFM-QCP (fixed temperature $\beta t = 12$); and (b) temperature T/t (fixed $r_0 = r_c$ at the AFM-QCP). The particle-hole symmetric dispersion used here is that of Fig. 1(b).

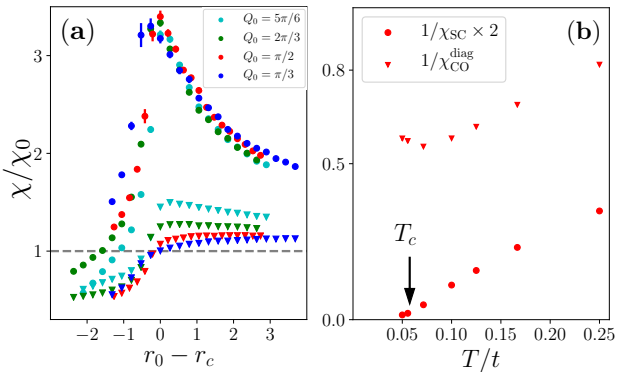

Figure 3. (a) SC (circles) and diagonal CO (triangles) susceptibilities, normalized by their non-interacting values, as a function of the distance to the QCP $r_0 - r_c$ and for a fixed temperature $\beta t = 10$. The dispersion is represented in Fig. 1(c), with different values of the wave-vector Q_0 (shown in the inset). Panel (b) shows the temperature dependence of the inverse susceptibilities at the AFM-QCP ($r_0 = r_c$) for $\mu/t = -\sqrt{2}$ ($Q_0 = \pi/2$).

We now proceed to investigate whether there is a remnant near-degeneracy between SC and CO when particle-hole symmetry is broken ($\mu \neq 0$). In this case, although there is no lattice SU(2) symmetry, an approximate SU(2) symmetry of the low energy theory near the hot spots is preserved [37][39]. To favor the CO state, we consider one-dimensional dispersions ($t_y = 0$), as shown in Fig. 1(c), although the results are similar for finite t_y (see Supplementary Material). To be able to assess the relevant CO wave-vectors $\mathbf{Q}_{\text{CO}} = (Q_0, Q_0)$ in the finite-

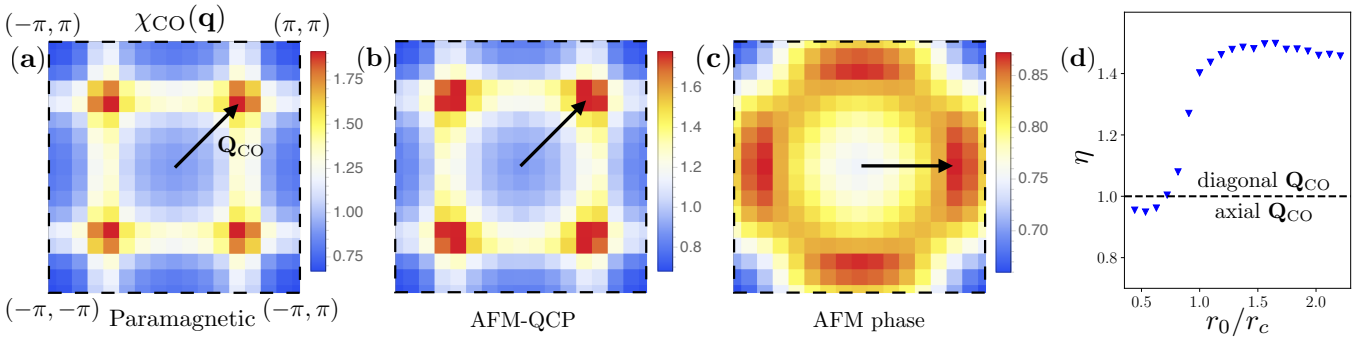

Figure 4. Panels (a)-(c) show the momentum dependence of the CO susceptibility $\chi_{\rm CO}(\mathbf{q})$ in the paramagnetic phase $r_0 = 2.2r_c$ (a), at the QCP (b), and in the AFM phase $r_0 = 0.44r_c$ (c). The dispersion is represented in Fig. 1(c) with $\mu/t = -\sqrt{2}$. (d) Ratio η of the maximum values of $\chi_{\rm CO}(\mathbf{q})$ along the diagonal direction, $\mathbf{q} = (q, q)$, and along the axial direction, $\mathbf{q} = (q, 0)$, for different inverse temperatures β (inset), as function of the distance to the QCP at $r_0 = r_c$. The dashed line at $\eta = 1$ marks the location where the maximum of the CO susceptibility changes between diagonal and axial directions. The results are obtained for $\beta t = 14$ and $L = 16$.

size QMC simulations, we choose μ values that yield commensurate $Q_0 \equiv 2\arccos\frac{-\mu}{2t} = \frac{2\pi n}{L}$, with $n = 2, 3, 4, 5$.

Figure 3(a) displays the behavior of $\chi_{\rm SC}$ and $\chi_{\rm CO}^{\rm diag}$, normalized by their non-interacting ($\lambda = 0$) value, as a function of the distance to the QCP for different values of μ. While the sharp enhancement of $\chi_{\rm SC}$ at $r_0 = r_c$ is preserved, the enhancement of $\chi_{\rm CO}^{\rm diag}$ is small for $r_0 > r_c$. This enhancement of $\chi_{\rm CO}^{\rm diag}$ is larger the closer μ is to zero, i.e. the closer the global lattice SU(2) symmetry is to be restored. The CO-SC degeneracy observed for $\mu = 0$ is absent, with SC clearly winning over CO. The competition between the two orders is highlighted in Fig. 3(b), where the T dependences of $1/\chi_{\rm SC}$ and $1/\chi_{\rm CO}^{\rm diag}$ are plotted at the QCP, $r_0 = r_c$. Interestingly, right above the Berezinskii-Kosterlitz-Thouless superconducting transition temperature T_c (extracted from the superfluid density, see Ref. [35]), $\chi_{\rm CO}^{\rm diag}$ reverses its trend and starts to decrease upon lowering the temperature. This provides evidence that the competition between SC and CO takes place already in the fluctuating regime.

Another important result from our QMC simulations is that, when the AFM hot spots are near the antinodal region of the Brillouin zone (i.e., $(\pi, 0)$ / $(0, \pi)$), the CO wave-vector tends to shift from diagonal to axial inside the AFM phase. To illustrate this, in Fig. 4 we plot $\chi_{\rm CO}(\mathbf{q})$ for the system with $\mu/t = -\sqrt{2}$ ($Q_0 = \pi/2$). Results for other fillings are discussed in the Supplementary Material. The tendency of shifting $\mathbf{Q}_{\rm CO}$ from diagonal (paramagnetic phase) to axial (AFM phase) is evident. To quantify this behavior, we plot in Fig. 4(d) the ratio between the maxima of $\chi_{\rm CO}$ along the diagonal and axial directions as function of r_0 for $\beta t = 14$. The maximum is along the diagonal direction in the paramagnetic phase. Inside the AFM phase, however, the maximum quickly shifts to the axial direction. This effect is consistent with theoretical proposals that axial CO is favored over diagonal CO if the antinodal regions of the Brillouin zone are gapped either by AFM order discussed here or by a more exotic pseudogap state [33, 34].

In summary, we showed that the spin-fermion model with particle-hole symmetric bands has an exact SU(2) symmetry that relates d-wave SC and d-wave CO. The breaking of this symmetry at the lattice level strongly suppresses the CO susceptibility, even though it remains a low-energy symmetry near the hot spots. Compared with previous QMC investigations of the spin-fermion model, which showed that the SC instability is governed by the hot spots [35], our results indicate that the CO instability is instead governed by the full electronic dispersion. Such an asymmetry between CO and SC implies that CO is not a universal phenomenon associated with AFM quantum criticality, in contrast to SC. The fragility of the SC-CO symmetry can be understood in renormalization group language. At the fixed point with a high emergent symmetry, small symmetry-breaking perturbations are strongly relevant [40], and quickly drive the system away from the high symmetry regime. The high symmetry may yet emerge at very low energies in an ideal, weak-coupling critical point. At a finite value of the coupling constant, however, interactions between degrees of freedom at different energy scales leads to a loss of the emergent symmetry. The SC channel wins because it is enhanced by both high and low energy degrees of freedom, in contrast to density-wave like instabilities.

The applicability of these results to specific materials – and particularly the cuprates – remains an open question. On the one hand, the CO observed in most cuprates only acquires a substantially long correlation length once SC is fully suppressed, and CO fluctuations are found to be suppressed by the onset of SC [8, 18, 19]. Furthermore, in the pseudogap state where CO is experimentally observed, the CO wave-vector is axial, and not diagonal. All these observations seem at least qual-

itatively consistent with our results for systems without particle-hole symmetric band dispersions. On the other hand, in hole-doped cuprates, AFM fluctuations become weaker as the system approaches optimal doping and CO is observed. The fact that CO is strongest near a specific doping close to 1/8, where AFM fluctuations are not particularly enhanced, suggests that lattice commensuration effects, rather than AFM criticality, may play an important role in these systems.

We thank A. Chubukov for fruitful discussions. X.W. and R.M.F. were supported by the U.S. Department of Energy, Office of Science, Basic Energy Sciences, under Award number DE-SC0012336. R.M.F. also acknowledges partial support from the Research Corporation for Science Advancement via the Cottrell Scholar Award, and X.W. acknowledges support from the Doctoral Dissertation Fellowship offered by the University of Minnesota. Y.W. is supported by the Gordon and Betty Moore Foundation's EPiQS Initiative through Grant No. GBMF4305 at the University of Illinois. Y.S is supported by the Department of Energy, Office of Science, Basic Energy Sciences, Materials Sciences and Engineering Division, under Contract DEAC02-76SF00515. R.M.F. and X.W. thank the Minnesota Supercomputing Institute (MSI) at the University of Minnesota, where part of the numerical computations was performed.

[1] D. J. Scalapino, Rev. Mod. Phys. **84**, 1383 (2012).
[2] M. A. Metlitski and S. Sachdev, New Journal of Physics **12**, 105007 (2010).
[3] M. A. Metlitski and S. Sachdev, Phys. Rev. B **82**, 075128 (2010).
[4] K. B. Efetov, H. Meier, and C. Pepin, Nat Phys **9**, 442 (2013).
[5] Y. Wang and A. Chubukov, Phys. Rev. B **90**, 035149 (2014).
[6] A. Allais, J. Bauer, and S. Sachdev, Phys. Rev. B **90**, 155114 (2014).
[7] T. Wu, H. Mayaffre, S. Kramer, M. Horvatic, C. Berthier, W. N. Hardy, R. Liang, D. A. Bonn, and M.-H. Julien, Nature **477**, 191 (2011).
[8] J. Chang, E. Blackburn, A. T. Holmes, N. B. Christensen, J. Larsen, J. Mesot, R. Liang, D. A. Bonn, W. N. Hardy, A. Watenphul, M. v. Zimmermann, E. M. Forgan, and S. M. Hayden, Nat Phys **8**, 871 (2012).
[9] A. J. Achkar, R. Sutarto, X. Mao, F. He, A. Frano, S. Blanco-Canosa, M. Le Tacon, G. Ghiringhelli, L. Braicovich, M. Minola, M. Moretti Sala, C. Mazzoli, R. Liang, D. A. Bonn, W. N. Hardy, B. Keimer, G. A. Sawatzky, and D. G. Hawthorn, Phys. Rev. Lett. **109**, 167001 (2012).
[10] G. Ghiringhelli, M. Le Tacon, M. Minola, S. Blanco-Canosa, C. Mazzoli, N. B. Brookes, G. M. De Luca, A. Frano, D. G. Hawthorn, F. He, T. Loew, M. M. Sala, D. C. Peets, M. Salluzzo, E. Schierle, R. Sutarto, G. A. Sawatzky, E. Weschke, B. Keimer, and L. Braicovich, Science **337**, 821 (2012).
[11] E. Blackburn, J. Chang, M. Hücker, A. T. Holmes, N. B. Christensen, R. Liang, D. A. Bonn, W. N. Hardy, U. Rütt, O. Gutowski, M. v. Zimmermann, E. M. Forgan, and S. M. Hayden, Phys. Rev. Lett. **110**, 137004 (2013).
[12] N. Doiron-Leyraud, S. Lepault, O. Cyr-Choinière, B. Vignolle, G. Grissonnanche, F. Laliberté, J. Chang, N. Barišić, M. K. Chan, L. Ji, X. Zhao, Y. Li, M. Greven, C. Proust, and L. Taillefer, Phys. Rev. X **3**, 021019 (2013).
[13] D. LeBoeuf, S. Kramer, W. N. Hardy, R. Liang, D. A. Bonn, and C. Proust, Nat Phys **9**, 79 (2013).
[14] R. Comin, A. Frano, M. M. Yee, Y. Yoshida, H. Eisaki, E. Schierle, E. Weschke, R. Sutarto, F. He, A. Soumyanarayanan, Y. He, M. Le Tacon, I. S. Elfimov, J. E. Hoffman, G. A. Sawatzky, B. Keimer, and A. Damascelli, Science **343**, 390 (2014).
[15] K. Fujita, C. K. Kim, I. Lee, J. Lee, M. H. Hamidian, I. A. Firmo, S. Mukhopadhyay, H. Eisaki, S. Uchida, M. J. Lawler, E.-A. Kim, and J. C. Davis, Science **344**, 612 (2014).
[16] E. H. da Silva Neto, P. Aynajian, A. Frano, R. Comin, E. Schierle, E. Weschke, A. Gyenis, J. Wen, J. Schneeloch, Z. Xu, S. Ono, G. Gu, M. Le Tacon, and A. Yazdani, Science **343**, 393 (2014).
[17] A. Mesaros, K. Fujita, S. D. Edkins, M. H. Hamidian, H. Eisaki, S.-i. Uchida, J. C. S. Davis, M. J. Lawler, and E.-A. Kim, Proceedings of the National Academy of Sciences **113**, 12661 (2016).
[18] H. Jang, W.-S. Lee, H. Nojiri, S. Matsuzawa, H. Yasumura, L. Nie, A. V. Maharaj, S. Gerber, Y.-J. Liu, A. Mehta, D. A. Bonn, R. Liang, W. N. Hardy, C. A. Burns, Z. Islam, S. Song, J. Hastings, T. P. Devereaux, Z.-X. Shen, S. A. Kivelson, C.-C. Kao, D. Zhu, and J.-S. Lee, Proceedings of the National Academy of Sciences **113**, 14645 (2016).
[19] J. Chang, E. Blackburn, O. Ivashko, A. T. Holmes, N. B. Christensen, M. Hücker, R. Liang, D. A. Bonn, W. N. Hardy, U. Rütt, M. v. Zimmermann, E. M. Forgan, and S. M. Hayden, Nature Communications **7**, 11494 (2016).
[20] S. Bulut, W. A. Atkinson, and A. P. Kampf, Phys. Rev. B **88**, 155132 (2013).
[21] S. Sachdev and R. La Placa, Phys. Rev. Lett. **111**, 027202 (2013).
[22] L. E. Hayward, D. G. Hawthorn, R. G. Melko, and S. Sachdev, Science **343**, 1336 (2014).
[23] S. Caprara, C. Di Castro, G. Seibold, and M. Grilli, Phys. Rev. B **95**, 224511 (2017).
[24] K. Kawaguchi, Y. Yamakawa, M. Tsuchiizu, and H. Kontani, Journal of the Physical Society of Japan **86**, 063707 (2017).
[25] M. Tsuchiizu, K. Kawaguchi, Y. Yamakawa, and H. Kontani, arXiv:1705.05356.
[26] W. Atkinson, S. Ufkes, and A. P. Kampf, arXiv:1710.08881.
[27] E. Berg, M. A. Metlitski, and S. Sachdev, Science **338**, 1606 (2012).
[28] A. Abanov, A. V. Chubukov, and J. Schmalian, Advances in Physics **52**, 119 (2003).
[29] Y. Schattner, M. H. Gerlach, S. Trebst, and E. Berg, Phys. Rev. Lett. **117**, 097002 (2016).
[30] H. Meier, C. Pépin, M. Einenkel, and K. B. Efetov, Phys. Rev. B **89**, 195115 (2014).
[31] D. Chowdhury and S. Sachdev, Phys. Rev. B **90**, 134516

(2014).
[32] Z.-X. Li, F. Wang, H. Yao, and D.-H. Lee, Phys. Rev. B **95**, 214505 (2017).
[33] D. Chowdhury and S. Sachdev, Phys. Rev. B **90**, 245136 (2014).
[34] W. A. Atkinson, A. P. Kampf, and S. Bulut, New Journal of Physics **17**, 013025 (2015).
[35] X. Wang, Y. Schattner, E. Berg, and R. M. Fernandes, Phys. Rev. B **95**, 174520 (2017).
[36] M. H. Gerlach, Y. Schattner, E. Berg, and S. Trebst, Phys. Rev. B **95**, 035124 (2017).
[37] Y. Wang, D. F. Agterberg, and A. Chubukov, Phys. Rev. B **91**, 115103 (2015).
[38] A. Moreo and D. J. Scalapino, Phys. Rev. Lett. **66**, 946 (1991).
[39] Technically the hot-spots symmetry is SU(2)$\times$ SU(2)$\sim$SO(4) and not SU(2), because for $\mu \neq 0$ the CO order parameter is complex, giving rise to a four-component super-vector.
[40] E. Fradkin, S. A. Kivelson, and J. M. Tranquada, Rev. Mod. Phys. **87**, 457 (2015).